RSC Advances

PAPER

View Article Online
View Journal | View Issue

Cite this: *RSC Adv.*, 2017, **7**, 43648

Extremely low coercivity in Fe_3O_4 thin film grown on Mg_2TiO_4 (001)

X. H. Liu,*[ab] W. Liu[b] and Z. D. Zhang[b]

Received 12th August 2017
Accepted 14th August 2017

DOI: 10.1039/c7ra08916c

rsc.li/rsc-advances

We report very different magnetic properties of 40 nm-thick Fe_3O_4 thin films grown on tailored spinel substrate Mg_2TiO_4 (001) and on general substrate MgO (001). The sample on Mg_2TiO_4 (001) shows a very sharp Verwey transition with narrow hysteresis of only 0.5 K and a high transition temperature up to 126 K and, in particular, an extremely small coercivity as low as around 7 Oe from the Verwey transition to room temperature. This low coercivity is close to that of the single crystal bulk but several times smaller than that of the sample on MgO (001). Our work gives a first example of the magnetic properties in Fe_3O_4 thin film having higher Verwey transition than that of the single crystal bulk, which not only greatly expands our understanding about Fe_3O_4 but also provides a very good candidate for spintronic applications with quite low energy consumption.

I. Introduction

Magnetite (Fe_3O_4) is one of the most studied transition-metal oxides over the past several decades because of its rather unique and interesting set of magnetic and electrical properties, such as high Curie temperature (T_C = 858 K), relatively high saturation magnetization, small coercivity field[1,2] and theoretically predicted half-metallic character.[3,4] These properties make Fe_3O_4 very attractive for room temperature spintronic applications.[5–9] Especially, Fe_3O_4 is a highly correlated material that undergoes a first-order metal–insulator transition (known as the Verwey transition[10]) at T_V = 124 K, but the mechanism of this transition is still unclear though tremendous amount of work has been done. However, the unique properties, which are relevant for various device applications, have been very difficult to realize in thin film form due to the existence of growth defects (such as the anti-phase boundaries (APBs)) and chemical-off stoichiometry. The inevitable presence of APBs in Fe_3O_4 thin films generally results in some unusual magnetic and transport properties, such as unsaturated magnetization in high magnetic fields,[11,12] superparamagnetic behavior for epitaxial ultrathin films,[13,14] unsaturated negative magnetoresistance,[15–24] and very low Verwey temperature and quite broadened transition.[15–19,21,22,24–26] Therefore, previous work of Fe_3O_4 thin films grown on MgO, $MgAl_2O_4$, $SrTiO_3$ or Al_2O_3 substrates in fact only reported the extrinsic magnetic and transport properties.[11–26]

To overcome these negative aspects, very recently, Liu *et al.*[27] obtained exceptionally high quality epitaxial Fe_3O_4 thin films grown on tailor-made spinel $Co_{2-x-y}Mn_xFe_yTiO_4$ (001) substrates, which not only show the Verwey transition as sharp as the single crystal bulk but also present very high T_V up to 136.5 K. This work provides a completely new platform to further investigate the intrinsic physical properties of the magnetite.[27] The $Co_{2-x-y}Mn_xFe_yTiO_4$ substrates, however, are magnetic, which significantly restricts the study of the magnetic properties in these high-quality Fe_3O_4 thin films. Furthermore, up to now, all the investigations on the magnetic properties of Fe_3O_4 thin films are done in the films grown on the general substrates such as MgO, $MgAl_2O_4$, $SrTiO_3$ or Al_2O_3,[9,11,12,15–19,21,22,24] which only show lower T_V than that of the bulk due to the existence of microstructure defects. Therefore, to study the magnetic properties in Fe_3O_4 thin film with higher T_V than that of the bulk will greatly extend our understanding about the magnetite. To experimentally achieve this goal, based on the work in ref. 27, we carefully chose and made a new non-magnetic spinel substrate Mg_2TiO_4 (001) with small lattice mismatch +0.51%. We expect that the Fe_3O_4 thin film grown this substrate will present higher T_V than that of the bulk and exhibit quite different magnetic properties from that of the films grown on the general substrates.

In this work, we report very different magnetic properties of 40 nm-thick Fe_3O_4 thin films grown on Mg_2TiO_4 (001) and MgO (001) substrates. It is found that the sample on Mg_2TiO_4 (001) displays a very sharp Verwey transition with narrow hysteresis of 0.5 K and a high T_V of 126 K, and remarkably an extremely small coercivity as low as around 7 Oe from Verwey transition to room temperature. This so low coercivity is close to that of the single crystal bulk but several times smaller than that of the sample on MgO (001), which makes Fe_3O_4/Mg_2TiO_4 (001) a very good candidate for spintronic applications in quite low energy consumption.

[a]*Max Planck Institute for Chemical Physics of Solids, Nöthnitzerstr. 40, 01187, Dresden, Germany. E-mail: xhliu@alum.imr.ac.cn*

[b]*Shenyang National Laboratory for Materials Science, Institute of Metal Research, Chinese Academy of Sciences, Shenyang 110016, China*

II. Experiments

The 40 nm-thick Fe_3O_4 thin films were grown on Mg_2TiO_4 (001) and MgO (001) substrates by using molecular beam epitaxy (MBE) in an ultrahigh vacuum system with a background pressure of 1×10^{-10} mbar range. The substrates were annealed for 2 h at 600 °C in an oxygen pressure of 3×10^{-7} mbar to obtain a clean and well-ordered surface structure before the deposition of Fe_3O_4. Standard samples were grown using an iron flux of 1 Å per minute, an oxygen background pressure of 1×10^{-6} mbar, and a growth temperature of 250 °C.[26] To determine the structural quality and chemical states, the films were analyzed *in situ* by using reflection high-energy electron diffraction (RHEED), low-energy electron diffraction (LEED) and X-ray photoemission spectroscopy (XPS). The RHEED patterns were taken at 20 keV electron energy, with the beam aligned parallel to the [100] direction of the substrate. The LEED patterns were recorded at electron energy of 88 eV. The thickness of the film was determined during growth from the oscillation period of the RHEED specular spot intensity. The XPS data were collected using 1486.6 eV photons (monochromatized Al K_α light) in normal emission geometry and at room temperature using a Scienta R3000 electron energy analyzer. The overall energy resolution was set to about 0.3 eV. The transport and magnetic properties of the Fe_3O_4 thin films were *ex situ* measured with a standard four probe technique using a physical property measurement system (PPMS) and superconducting quantum interference device (SQUID), respectively. High-resolution X-ray diffraction (HR-XRD) was employed for further *ex situ* investigation of the structural quality and the microstructure of the thin films. The XRD measurements were performed with a high resolution PANalytical X'Pert MRD diffractometer using monochromatic Cu $K_{\alpha 1}$ radiation ($\lambda = 1.54056$ Å).

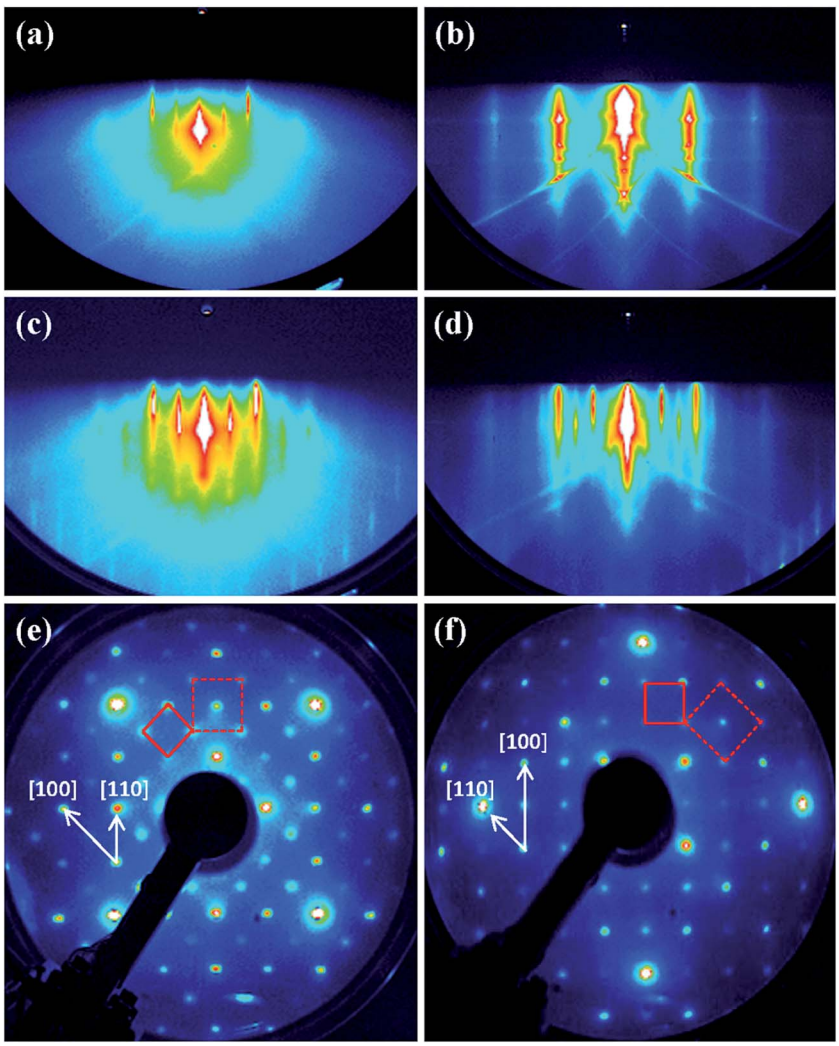

Fig. 1 RHEED and LEED electron diffraction patterns of the following: the clean substrates Mg_2TiO_4 (001) (a) and MgO (b); 40 nm-thick Fe_3O_4 thin films grown on Mg_2TiO_4 (001) (c) and (e), and on MgO (001) (d) and (f), respectively. The (1×1) unit cell and the $(\sqrt{2} \times \sqrt{2})R45°$ superlattice are indicated by the red dashed square and solid square, respectively.

III. Results and discussions

Fig. 1 shows the RHEED electron diffraction patterns of clean substrates Mg_2TiO_4 (001) (a) and MgO (001) (b), the RHEED and LEED patterns of 40 nm-thick Fe_3O_4 thin films grown on Mg_2TiO_4 (001) (c and e), and on MgO (001) (d and f), respectively. The sharp RHEED streaks and the presence of Kikuchi lines (Fig. 1(c) and (d)), as well as the high contrast and sharp LEED spots (Fig. 1(e) and (f)) indicate a flat and well ordered (001) single crystalline surface structure of both samples. The characteristic $(\sqrt{2} \times \sqrt{2})R45^\circ$ surface reconstruction of Fe_3O_4 (001) can be observed, providing another indication for the high structural quality of the two Fe_3O_4 thin films. The (1×1) unit cell and the $(\sqrt{2} \times \sqrt{2})R45^\circ$ superlattice are indicated by the red dashed square and solid square, respectively (see Fig. 1(e) and (f)).[28,29] Moreover, it is found that the LEED pattern for the film on Mg_2TiO_4 (001) has 45° rotation as compared to the film on MgO (001), which should be due to the direction rotation of the substrate during its production process. Furthermore, to clarify the chemical states of the iron oxide, the thin films were *in situ* analyzed by XPS, as shown in Fig. 2(a)–(c). It is clear that the two samples exhibit the same wide scan spectra with binding energy from 1200 to −18 eV (Fig. 2(a)), Fe 2p core-level spectra (Fig. 2(b)) and valence band spectra (Fig. 2(c)), which demonstrates quite clean surface of the thin films and represents the typical signatures of Fe_3O_4 thin film.[26,27,30,31] The structural quality of the thin films was further *ex situ* investigated by the high-resolution X-ray diffraction (HR-XRD). As shown in the Fig. 2(d), the long range θ–2θ XRD patterns do not present any phase other than Fe_3O_4, the (002)/(004) and (004)/(008) reflections correspond to MgO/Fe_3O_4 because of the lattice constant of Fe_3O_4 as twice as that of MgO (see the green color curve), and the (004) and (008) reflections are presented for both Mg_2TiO_4 and Fe_3O_4 for the red color curve. The two samples are in fully strained due to the small lattice mismatches.[27,32] As the lattice mismatch of Mg_2TiO_4 (+0.51%) is larger than that of MgO (+0.33%), the tensile strain and also the lattice constant a (in-plane) are bigger for the former, and thus the lattice constant c (out-of-plane) of the Fe_3O_4/Mg_2TiO_4 (001) (8.343 Å) is smaller than that of the Fe_3O_4/MgO (001) (8.367 Å), corresponding to the relative shift of (004) and (008) peaks to the larger angles (see the red curve).

The resistivity as a function of temperature $\rho(T)$ of 40 nm-thick Fe_3O_4 thin films grown on Mg_2TiO_4 (001) and MgO (001), and of single crystal bulk is shown in Fig. 3(a). It is found that the $\rho(T)$ curves present a clear first-order Verwey transition. The Fe_3O_4/MgO (001) sample displays a low T_V with a big hysteretic loop of about 4 K whereas the Fe_3O_4/Mg_2TiO_4 (001) sample exhibits a higher T_V (126 K) than that of the bulk with very narrow hysteresis of only 0.5 K, which demonstrates that

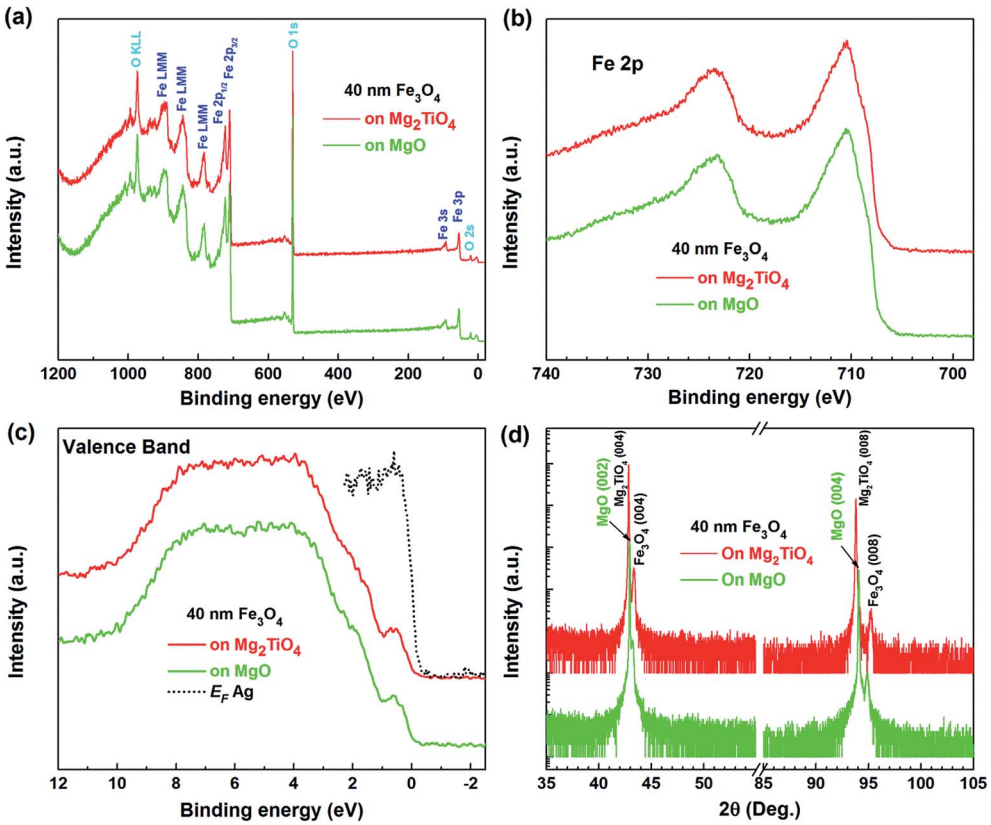

Fig. 2 XPS spectra of 40 nm-thick Fe_3O_4 thin films grown on Mg_2TiO_4 (001) and MgO (001): wide scan spectra (a), Fe 2p core-level spectra (b) and valence band spectra, as well as Ag for reference (c); (d) X-ray diffraction patterns for the Fe_3O_4 thin films on Mg_2TiO_4 (001) and MgO (001). Only the (004) and (008) reflections of Fe_3O_4 can be observed for the two samples.

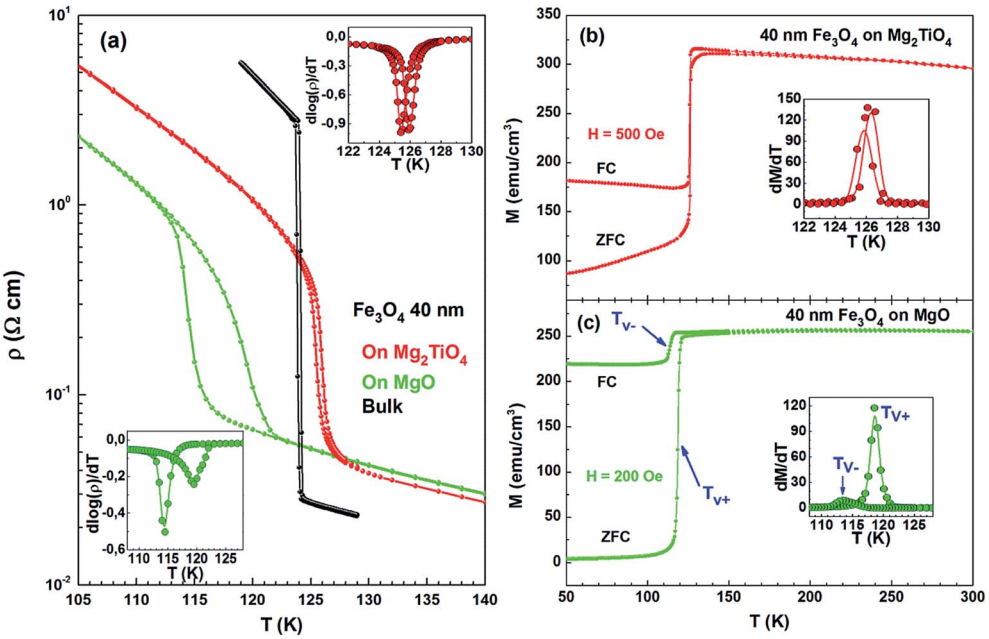

Fig. 3 Resistivity as a function of temperature for 40 nm-thick Fe_3O_4 thin films on Mg_2TiO_4 (001) and MgO (001), and of single crystal bulk Fe_3O_4 (a). Inset: temperature dependence of d$\log(\rho)$/dT near the T_V for the samples on Mg_2TiO_4 (001) (up) and MgO (001) (down), respectively; zero-field-cooling (ZFC) and field-cooling (FC) magnetization of the samples on Mg_2TiO_4 (001) (b) and MgO (001) (c), respectively. The dM/dT *versus* temperature around the T_V for the thin films on Mg_2TiO_4 (001) and MgO (001) are displayed as insets of (b) and (c), respectively.

the Fe_3O_4/Mg_2TiO_4 (001) sample has quite few microstructural defects and the tensile strain pushes the T_V over that of the bulk.[27] The temperature dependence of magnetization $M(T)$ of 40 nm-thick Fe_3O_4 thin films on Mg_2TiO_4 (001) and MgO (001) are exhibited in Fig. 3(b) and (c), respectively. It is obvious that a sharp jump of magnetization takes place at Verwey transition. The T_{V-} and T_{V+} are defined respectively as the temperature of the maximum slop of $\log(\rho(T))$ or $M(T)$ curve for the cooling down and warming up temperature branches. Clearly, the T_{V+} and T_{V-} from the zero-field-cooling (ZFC) and field-cooling (FC) $M(T)$ curves in Fig. 3(b) and (c) are consistent with that from $\rho(T)$ curves in Fig. 3(a) (see the insets of Fig. 3(a)–(c)). Furthermore, it is found that the FC curve of Fe_3O_4/Mg_2TiO_4 (001) film shows much larger magnetization change at T_{V-} than that of Fe_3O_4/MgO (001) film (see Fig. 3(b) and (c)). Although the bulk Fe_3O_4 keeps ferrimagnetic below $T_C \sim 860$ K, yet the easy (hard) axis changes from [111] ([100]) to [100] ([111]) with changing from cubic $Fd\bar{3}m$ to monoclinic Cc.[33,34] Usually, the bulk Fe_3O_4 exhibits a very sharp variation of magnetization at T_V under small magnetic field.[35] In Fe_3O_4 thin films, however, the presence of microstructure defects can negatively affect the rotation of the magnetic axis. Therefore, the Fe_3O_4/Mg_2TiO_4 (001) film having fewer microstructure defects is more sensitive to the applied magnetic field, and the much larger magnetization change at T_{V-} can be observed.

It has been reported that the coercivity field (H_C) significantly enhances with the Fe_3O_4 transforming from high-temperature cubic spinel structure to low-temperature monoclinic structure due to the abrupt increase in magnetocrystalline and magnetostriction constants.[35–38] The in-plane magnetic hysteresis loops at 126 K (at T_V) and 127 K (just above T_V) in applied field of 50 kOe of the 40 nm Fe_3O_4/Mg_2TiO_4 (001) film is shown in Fig. 4(a). It is observed that the H_C sharply decreases from 213 Oe at 126 K to only 6 Oe at 127 K (see the inset (left) of Fig. 4(a)). Remarkably, this extremely small H_C at 127 K, to our knowledge, is the smallest value in Fe_3O_4 thin films so far, which is close to that of the single crystal bulk[36] but several times smaller than that reported in thin films grown on MgO, $MgAl_2O_4$, $SrTiO_3$ or Al_2O_3.[9,15,16,19,21,22,24,37,38] Moreover, near the H_C, a clear incoherent reversal of magnetization with magnetic field for 126 K while a rapid jump of magnetization with magnetic field for 127 K are observed, see the sharp peak of d(M/M_S)/dH at 127 K in the inset (right) of Fig. 4(a).

The in-plane H_C as a function of temperature for 40 nm-thick Fe_3O_4 thin films on Mg_2TiO_4 (001) and MgO (001) are plotted in Fig. 4(c). A sharp change of H_C occurs at their Verwey transitions for the two samples, respectively. Especially, the Fe_3O_4/Mg_2TiO_4 (001) sample keeps nearly constant H_C of only about 7 Oe above its T_V. As a contrast, the values of H_C are much larger for the Fe_3O_4/MgO (001) sample, ranging from 140 Oe at 130 K to 90 Oe at 300 K and still about two times bigger than that of the Fe_3O_4/Mg_2TiO_4 (001) sample at low temperatures ($T < T_V$). Furthermore, the two samples present the perpendicular anisotropic behavior, that the in-plane and out-of-plane correspond to the easy and hard axis, respectively (see Fig. 4(b)), and the anisotropic field is about 5 kOe, similar to that reported in previous work.[20,39] It has been known that the microstructural defects (such as the APBs) greatly affect the transport and magnetic properties of Fe_3O_4 thin films, the APBs were claimed to act as pining centers for the magnetic domain walls,[37] thus the substantial enhancement of H_C for the Fe_3O_4/MgO (001) film should be

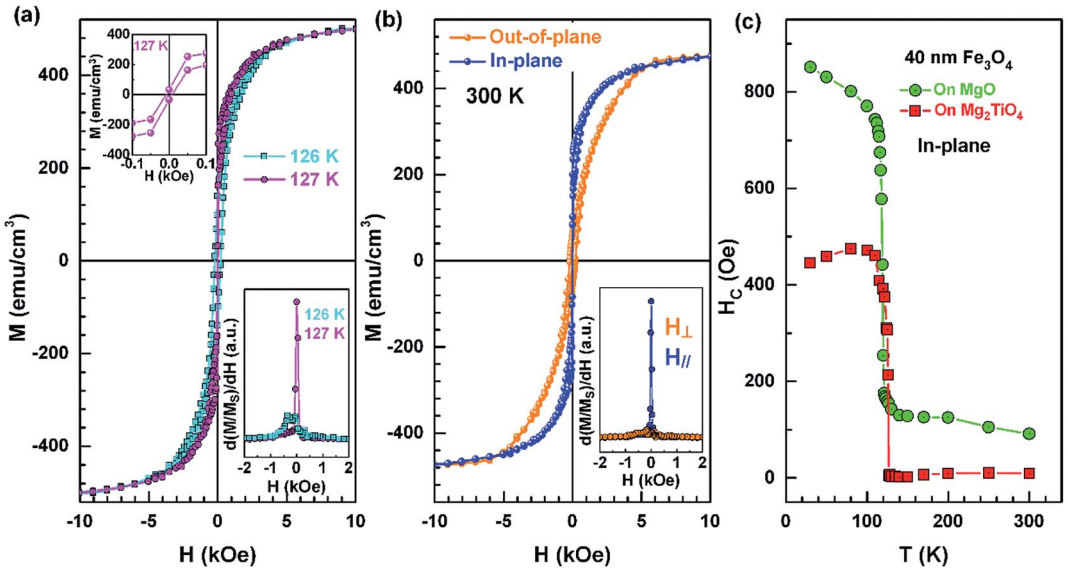

Fig. 4 (a) In-plane magnetic hysteresis loops in applied field of 50 kOe for 40 nm-thick Fe_3O_4 thin film grown on Mg_2TiO_4 (001) at 126 (at T_V) and 127 K (just above T_V). Inset: (left) magnetic hysteresis loop under small magnetic field 0.1 kOe at 127 K; (right) $d(M/M_S)/dH$ as a function of magnetic field around the H_C; (b) in-plane and out-of-plane magnetic hysteresis loops of the sample on Mg_2TiO_4 (001) at 300 K. Inset: $d(M/M_S)/dH$ *vs.* H around the H_C; (c) temperature dependence of H_C (in-plane) for 40 nm-thick Fe_3O_4 thin films on Mg_2TiO_4 (001) and MgO (001). A sharp change of H_C can be seen at their Verwey transitions and the values of H_C for the sample on Mg_2TiO_4 (001) are much smaller than that of the sample on MgO (001).

induced from this effect. As a result, by using a tailored spinel substrate we can obtain exceptionally high quality Fe_3O_4 thin film, with getting rid of the microstructure defects, it is the first time for us to observe the magnetic properties in Fe_3O_4 thin film having higher T_V than that of the single crystal bulk, which enlarges our understanding about the Fe_3O_4. Furthermore, this Fe_3O_4/Mg_2TiO_4 (001) thin film with extremely low coercivity will bring in quite low energy consumption in spin valves or spin tunnel junctions.

IV. Conclusion

In summary, we have studied the magnetic properties of 40 nm-thick Fe_3O_4 thin films grown on Mg_2TiO_4 (001) and on MgO (001). We found that the Fe_3O_4/Mg_2TiO_4 (001) film shows a very sharp Verwey transition with narrow hysteresis and high T_V up to 126 K, and especially an extremely small H_C as low as about 7 Oe from the Verwey transition to room temperature. This small H_C is close to that of the single crystal bulk but several times smaller than that of the films grown on general substrates. Our work not only gives a first example of the magnetic properties in Fe_3O_4 thin film having higher Verwey transition than that of the single crystal bulk but also provides a very good candidate for spintronic applications in quite low energy consumption.

Conflicts of interest

There are no conflicts to declare.

Acknowledgements

The authors would like to thank Prof. Liu Hao Tjeng, Dr Chun-Fu Chang and Dr Alexander Komarek for useful discussion. This work has been supported by the Max Planck-POSTECH Center for Complex Phase Materials, and the National Basic Research Program of China (No. 2017YFA0206302), and the National Nature Science Foundation of China under projects 51590883 and 51331006, and as a project of the Chinese Academy of Sciences with grant number KJZD-EW-M05-3.

References

1 F. Walz, The Verwey transition – a topical review, *J. Phys.: Condens. Matter*, 2002, **14**, R285–R340.
2 J. Garcia and G. Subias, The Verwey transition – a new perspective, *J. Phys.: Condens. Matter*, 2004, **16**, R145–R178.
3 R. A. de Groot, F. M. Mueller, P. G. van Engen and K. H. J. Buschow, New Class of Materials: Half-Metallic Ferromagnets, *Phys. Rev. Lett.*, 1983, **50**, 2024–2027.
4 A. Yanase and K. Siratori, Band structure in the high temperature phase of Fe_3O_4, *J. Phys. Soc. Jpn.*, 1984, **53**, 312–317.
5 X. W. Li, A. Gupta, G. Xiao, W. Qian and V. P. Dravid, Fabrication and properties of heteroepitaxial magnetite (Fe_3O_4) tunnel junctions, *Appl. Phys. Lett.*, 1998, **73**, 3282–3284.
6 G. Hu and Y. Suzuki, Negative Spin Polarization of Fe_3O_4 in Magnetite/Manganite-Based Junctions, *Phys. Rev. Lett.*, 2002, **89**, 276601.

7 L. M. B. Alldredge, R. V. Chopdekar, B. B. Nelson-Cheeseman and Y. Suzuki, Spin-polarized conduction in oxide magnetic tunnel junctions with spinel/perovskite interfaces, *Appl. Phys. Lett.*, 2006, **89**, 182504.

8 T. Kado, Large room-temperature inverse magnetoresistance in tunnel junctions with a Fe_3O_4 electrode, *Appl. Phys. Lett.*, 2008, **92**, 092502.

9 J. B. Moussy, From epitaxial growth of ferrite thin films to spin-polarized tunneling, *J. Phys. D: Appl. Phys.*, 2013, **46**, 143001.

10 E. J. W. Verwey, Electronic conduction of magnetite (Fe_3O_4) and its transition point at low temperatures, *Nature*, 1939, **144**, 327–328.

11 D. T. Margulies, F. T. Parker, F. E. Spada, R. S. Goldman, J. Li, R. Sinclair and A. E. Berkowitz, Anomalous moment and anisotropy behavior in Fe_3O_4 films, *Phys. Rev. B*, 1996, **53**, 9175–9187.

12 D. T. Margulies, F. T. Parker, M. L. Rudee, F. E. Spada, J. N. Chapman, P. R. Aitchison and A. E. Berkowitz, Origin of the Anomalous Magnetic Behavior in Single Crystal Fe_3O_4 Films, *Phys. Rev. Lett.*, 1997, **79**, 5162–5165.

13 F. C. Voogt, T. T. M. Palstra, L. Niesen, O. C. Rogojanu, M. A. James and T. Hibma, Superparamagnetic behavior of structural domains in epitaxial ultrathin magnetite films, *Phys. Rev. B: Condens. Matter Mater. Phys.*, 1998, **57**, R8107–R8110.

14 W. Eerenstein, T. Hibma and S. Celotto, Mechanism for superparamagnetic behavior in epitaxial Fe_3O_4 films, *Phys. Rev. B: Condens. Matter Mater. Phys.*, 2004, **70**, 184404.

15 G. Q. Gong, A. Gupta, G. Xiao, W. Qian and V. P. Dravid, Magnetoresistance and magnetic properties of epitaxial magnetite thin films, *Phys. Rev. B: Condens. Matter Mater. Phys.*, 1997, **56**, 5096–5099.

16 X. W. Li, A. Gupta, G. Xiao and G. Q. Gong, Transport and magnetic properties of epitaxial and polycrystalline magnetite thin films, *J. Appl. Phys.*, 1998, **83**, 7049–7051.

17 M. Ziese and H. J. Blythe, Magnetoresistance of magnetite, *J. Phys.: Condens. Matter*, 2000, **12**, 13–28.

18 M. Ziese, Extrinsic magnetotransport phenomena in ferromagnetic oxides, *Rep. Prog. Phys.*, 2002, **65**, 143–249.

19 M. Ziese, R. Hohne, H. C. Semmelhack, H. Reckentin, N. H. Hong and P. Esquinazi, Mechanism of grain-boundary magnetoresistance in Fe_3O_4 films, *Eur. Phys. J. B*, 2002, **28**, 415–422.

20 W. Eerenstein, T. T. M. Palstra, S. S. Saxena and T. Hibma, Spin-Polarized Transport across Sharp Antiferromagnetic Boundaries, *Phys. Rev. Lett.*, 2002, **88**, 247204.

21 S. K. Arora, R. G. S. Sofin and I. V. Shvets, Magnetoresistance enhancement in epitaxial magnetite films grown on vicinal substrates, *Phys. Rev. B: Condens. Matter Mater. Phys.*, 2005, **72**, 134404.

22 A. V. Ramos, J. B. Moussy, M. J. Guittet, A. M. Bataille, M. G. Soyer, M. Viret, C. Gatel, P. B. Guillemaud and E. Snoeck, Magnetotransport properties of Fe_3O_4 epitaxial thin films: Thickness effects driven by antiphase boundaries, *J. Appl. Phys.*, 2006, **100**, 103902.

23 A. F. Pacheco, J. Orna, J. M. De Teresa, P. A. Algarabel, L. Morellon, J. A. Pardo, M. R. Ibarra, E. Kampert and U. Zeitler, High-field Hall effect and magnetoresistance in Fe_3O_4 epitaxial thin films up to 30 Tesla, *Appl. Phys. Lett.*, 2009, **95**, 262108.

24 R. G. S. Sofin, S. K. Arora and I. V. Shvets, Positive antiphase boundary domain wall magnetoresistance in Fe(110) heteroepitaxial films, *Phys. Rev. B: Condens. Matter Mater. Phys.*, 2011, **83**, 134436.

25 W. Eerenstein, T. T. M. Palstra, T. Hibma and S. Celotto, Origin of the increased resistivity in epitaxial Fe_3O_4 films, *Phys. Rev. B: Condens. Matter Mater. Phys.*, 2002, **66**, 201101.

26 X. H. Liu, A. D. Rata, C. F. Chang, A. C. Komarek and L. H. Tjeng, Verwey transition in Fe_3O_4 thin films: Influence of oxygen stoichiometry and substrate-induced Microstructure, *Phys. Rev. B: Condens. Matter Mater. Phys.*, 2014, **90**, 125142.

27 X. H. Liu, C. F. Chang, A. D. Rata, A. C. Komarek and L. H. Tjeng, Fe_3O_4 thin films: controlling and manipulating an elusive quantum material, *npj Quantum Materials*, 2016, **1**, 16027.

28 F. Y. Ran, Y. Tsunemaru, T. Hasegawa, Y. Takeichi, A. Harasawa, K. Yaji, S. Kim and A. Kakizaki, Angle-resolved photoemission study of $Fe_3O_4(001)$ films across Verwey transition, *J. Phys. D: Appl. Phys.*, 2012, **45**, 275002.

29 W. Wang, J. M. Mariot, M. C. Richter, O. Heckmann, W. Ndiaye, P. De Padova, A. Taleb-Ibrahimi, P. Le Fèvre, F. Bertran, F. Bondino, E. Magnano, J. Krempasky, P. Blaha, C. Cacho, F. Parmigiani and K. Hricovini, Fe t_{2g} band dispersion and spin polarization in thin films of $Fe_3O_4(001)/MgO(001)$: Half-metallicity of magnetite revisited, *Phys. Rev. B: Condens. Matter Mater. Phys.*, 2013, **87**, 085118.

30 S. A. Chambers and S. A. Joyce, Surface termination, composition and reconstruction of $Fe_3O_4(001)$ and γ-$Fe_2O_3(001)$, *Surf. Sci.*, 1999, **420**, 111–122.

31 S. A. Chambers, R. F. C. Farrow, S. Maat, M. F. Toney, L. Folks, J. G. Catalano, T. P. Trainor and G. E. Brown Jr, Molecular beam epitaxial growth and properties of $CoFe_2O_4$ on MgO(001), *J. Magn. Magn. Mater.*, 2002, **246**, 124–139.

32 M. Luysberg, R. G. S. Sofin, S. K. Arora and I. V. Shvets, Strain relaxation in $Fe_3O_4/MgAl_2O_4$ heterostructures: Mechanism for formation of antiphase boundaries in an epitaxial system with identical symmetries of film and substrate, *Phys. Rev. B: Condens. Matter Mater. Phys.*, 2009, **80**, 024111.

33 B. A. Calhoun, Magnetic and Electric Properties of Magnetite at Low Temperatures, *Phys. Rev.*, 1954, **94**, 1577–1585.

34 Z. Kakol, Magnetic and transport properties of magnetite in the vicinity of the Verwey transition, *J. Solid State Chem.*, 1990, **88**, 104–114.

35 A. R. Muxworthy and E. McClelland, Review of the low-temperature magnetic properties of magnetite from a rock magnetic perspective, *Geophys. J. Int.*, 2000, **140**, 101–114.

36 A. R. Muxworthy, Low-temperature susceptibility and hysteresis of magnetite, *Earth Planet. Sci. Lett.*, 1999, **169**, 51–58.

37 A. Bollero, M. Ziese, R. Hohne, H. C. Semmelhack, U. Kohler, A. Setzer and P. Esquinazi, Influence of thickness on microstructural and magnetic properties in Fe_3O_4 thin films produced by PLD, *J. Magn. Magn. Mater.*, 2005, **285**, 279–289.

38 F. Delille, B. Dieny, J. B. Moussy, M. J. Guittet, S. Gota, M. G. Soyer and C. Marin, Study of the electronic paraprocess and antiphase boundaries as sources of the demagnetisation phenomenon in magnetite, *J. Magn. Magn. Mater.*, 2005, **294**, 27–39.

39 P. A. A. van der Heijden, M. G. van Opstal, C. H. W. Swuste, P. H. J. Bloemen, J. M. Gaines and W. J. M. de Jonge, A ferromagnetic resonance study on ultra-thin Fe_3O_4 layers grown on (0 0 1) MgO, *J. Magn. Magn. Mater.*, 1998, **182**, 71–80.